Journal of Radiation and Nuclear Applications
An International Journal

http://dx.doi.org/10.18576/jrna/060307

Radiological Impact of Natural Radioactivity and Excessive Lifetime Cancer Risk in Sedimentary Rock Samples from Farsh El Azraq Area, Sinai, Egypt

E. S. Abd El-Halim[*] *and Amira A.Shenoda*

Nuclear Physics Laboratory, Women Faculty for Art, Science and Education, Ain Shams University, Cairo, Egypt.

Received: 24 July. 2021, Revised: 27 July. 2021, Accepted: 16 Aug. 2021.
Published online: 1 September 2021.

Abstract: The primary goal of this research is to determine the activity concentrations (Bq/kg) of naturally occurring radionuclides ^{238}U, ^{226}Ra, ^{232}Th, and ^{40}K in various types of sedimentary rock samples from the Um Bogma Formation in Sinai's Farsh El Azraq district. The measurements were made using a coaxial HPGe detector and gamma-ray spectrometry. (Siltstone, variegated shale, marl and dolostone) are the samples under study. The activity ratios ^{226}Ra/^{238}U and ^{238}U/^{235}U were calculated to estimate the radioactive equilibrium/disequilibrium in the area under study. This study reveals in general that all samples are exceeding the world permissible safe criteria and consider a risk source for human environment.

Keywords: HPGe detector, Sedimentary rock, Excess lifetime cancer risk.

1 Introduction

The ^{238}U, ^{235}U, and ^{232}Th are the parents of the three natural decay series, each of which is made up of a large number of daughter products generated by the decay of parent radionuclides. ^{40}K is a radionuclide that decays through beta emission and then emits a gamma photon as a byproduct. The mass basis there is far more ^{238}U than ^{235}U in a natural sample, the activity ratio is approximately 21.7 **[**1**]**.

The radioactive sequence reaches secular equilibrium [2]. The Um Bogma Formation is divided into three members (lower, middle, and upper) for this analysis, with the name, type, and description of the samples displayed.

This study is represented by the Um Bogma Formation subdivided into three members (lower, middle and upper), where the name, type and description of the samples shown in Table (1).

The activity concentrations of background radionuclides ^{226}Ra, ^{232}Th, and ^{40}K in some sedimentary rocks from the Farsh El Azraq region in Sinai were calculated using gamma-ray spectrometry with an HPGe detector to estimate the doses originating from the presence of these radionuclides, and to Calculate the radiation doses and risks, as well as the effect on the environment.

and their decay products). The majority of naturally occurring radionuclides can be found in soil and rocks at concentrations that are safe for human health and the environment [3]. However, due to geological epochs, certain areas have a relatively high natural concentration of U, Ra, and Th.

Table 1: Samples name, type and Description.

Sample name	Sample type	Description
FAZ 1	Siltstone (lower member)	Reddish brown, ferruginous at the bottom, hosting Fe-Mn ore,compact,bedded at the top.
FAZ 2	Dolostone (upper member)	Grey, sucrose, the middle member is mudstone, pale gray to dark yellow, ferruginous and medium hard with Mn pockets.
FAZ 3	Siltstone (middle member)	Variegated in colour, ferruginous, medium hard with Mn pockets.
FAZ 4	Siltstone (middle member)	Variegated in colour, ferruginous, medium hard with kaolin at the base, yellow with black patches with sandstone lens, brown and coarse grained.
FAZ 5	Marl (middle member)	Soft with white kaolin patches and Mn pockets.
FAZ 6	Marl (middle member)	Dark yellow, soft, massive.

[*]Corresponding author e-mail: hrs27@yahoo.com

© 2021 NSP
Natural Sciences Publishing Cor.

Sample name	Sample type	Description
FAZ 7	Siltstone (middle member)	Reddish brown, highly ferruginous, medium hard with Mn pockets.
FAZ 8	Siltstone (middle member)	Reddish brown, ferruginous, medium hard.
FAZ 9	Variegated shale (middle member)	Reddish brown, violet, green, soft, with black gibbsite and boulder of dolostone embedded in the variegated shale.

*Each sample (FAZ) represent of average of 3 samples. (A, B, C) where, A-Base part, B- Middle part, C- Upper part of the layer formation.

2 Experimental Sections

2.1 Study Area

The research area (Fig. 1) is in Egypt's southwestern Sinai [4]. The samples are taken from a specific location; Farsh El Azraq is located at the intersection of longitude 33° 25' and latitude 29° 59', according to GPS. An environmental plan analysis was used to select the study location.

As shown in Fig. (2), these rock units can be classified in the lithostratigraphic section. Where the samples were collected, they represented the Lower Carboniferous Um Bogma format ion (325 million year).

The Um Bogma Formation is more significant than the others because it contains the majority of radioactive anomalies. It is divided into three members:

(1) Lower Shaly-Ore Member, which consists of black shale with thin sandy dolomite bands and manganese-iron ore; (2) Upper Shaly-Ore Member, which consists of black shale with thin sandy dolomite bands and manganese-iron ore; and (3) Upper Shaly-Ore Member, which consists It is introduced the lateritic profile section and the formation of gibbsite-bearing shale. This rock unit is highly radioactive when it is karstified and lateritized **[**6**]**.

(2) Marl with siltstone and gibbsite-bearing siltstone make up the Middle Marly Dolostone-Siltstone Member, which is also karstified and lateritized. It is 6–8 m thick and mildly radioactive.

(3) The Upper Dolostone Member is a bedded dolostone with thin shale interbeds that is unconformable overlying the karstified and lateritized soil profile.

2.2 *Sample Preparation for Natural Radioactivity*

In this technique, 9 samples are used, with each sample representing (average of 3 samples (A,B,C) of the layer formation, for a total of 27 samples of different types of sedimentary rocks collected from the Farsh El Azraq region in Sinai, as shown in the diagram Table **(1)**. The samples were cleaned, crushed, and sieved at a scale of 200 mesh. Samples were weighed and placed in polyethene bags.

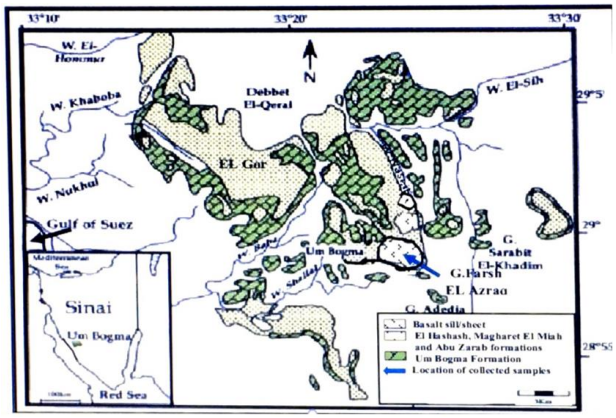

Fig. 1: Geologic map of the studied area of Um Bogma formation in southwestern Sinai, Egypt (Farsh AL-Azraq) area.

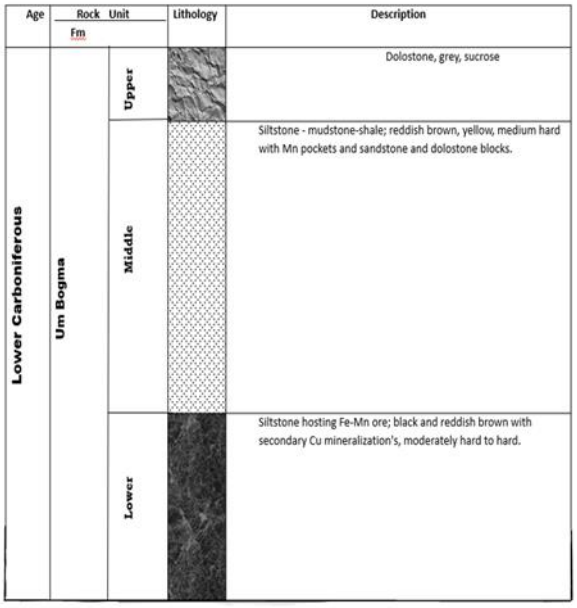

Fig.2: Lithostratigraphic section of southwestern Sinai in Um Bogma formation.

2.3 Radioactivity Measurements

2.3.1 Measurement Setup

To make it similar to a multi-channel analyzer, a high purity vertical germanium detector (HPGE) was coupled to a PC-computer with a special electronic card (MCA). The ORTEC hyper pure germanium (HPGe) detector, model GEM-15190, is a coaxial type detector with a serial number of 27-P-1876A. Negative 3KV is the suggested operating bias voltage.

A single germanium crystal with a length of 47.1mm and a diameter of 49.3mm was used in the detector. The HPGe

© 2021 NSP
Natural Sciences Publishing Cor.

detector has a complete width at half limit (FWHM) of 1.9 keV for the ^{60}Co gamma transition at 1332.5 keV and 0.9 keV for the ^{57}Co gamma transition at 122 keV. The peak to Compton ratio of the detector is about 44 KeV. The Compton ratio is calculated by dividing the number of net counts in the 1.33 MeV peak channels by the average.

A shaping amplifier, a preamplifier, and a high-voltage power supply are electronic devices that transform event energy into a pulse height range. The multi-channel analyzer converts the pulse amplitude into an equivalent amount (MCA). The data for the gamma-ray spectra was collected and analyzed using the

Germanium detectors must be cooled using an isolated Dewar in which a tank of liquid nitrogen (N_2) at temperature reduced to 77^{o}K **[**10**]**. The following gamma standard sources were used to calibrate the HPGe detector: ^{60}Co (1173.2 and 1332.5 KeV), ^{241}Am (59.5 KeV), and ^{226}Ra (185.7, 241.92, 351.99, and 609.70 KeV). In carrying out any measurement, attention has to be given to the fact that the source strength of the sample under investigation is comparable with that of the standard sources, in order to prevent errors caused by amplification shift The performance calibration of the HPGe detector was calculated using three well-known reference materials for U, Th, and K activity measurements obtained from the International Atomic Energy Agency (IAEA): RGU-1, RGTh-1, and RGK-1 [11, 12]. For counting, the sample containers were put on top of the detector.

The sample containers were placed on top of the detector for counting. The same geometry and size were used for both the samples and the reference materials **[**13**]**

The uranium reference material (RGU-1) is U-ore diluted with silica with 4940 Bq/Kg of ^{238}U, 228 Bq/Kg of ^{235}U, a negligible amount of ^{40}K (less than 0.63 Bq/Kg) and some traces of ^{232}Th (less than 4 Bq/Kg). The thorium reference material (RGTh-1) is Th-ore diluted with silica having 3250 Bq/Kg of ^{232}Th, but containing some ^{238}U (78 Bq/Kg) and ^{40}K (6.3 Bq/Kg). The potassium calibration reference material (RGK-1) is made from high purity (99.8%) potassium sulphate with 14000 Bq/Kg of potassium and uranium and thorium contents of less than 0.001 and 0.01 ppm, respectively [**10**]. To reduce the variability in gamma-ray intensities, as well as the effect of cascade summation and self-absorption effects of the emitted gamma photons, absolute efficiency calibration of the gamma spectrometry device was performed using the radionuclide basic efficiency method [**14**].

2.3.2 Data Analysis

The primordial ^{238}U is the most abundant isotope of U (99.27 %). It decays to ^{234}Th with the emission of α-particle. Through two consecutive β - transitions, ^{234}Th decays to ^{234m}Pa (half-lives of 24.10 days and 6.69 h, respectively) and to ^{234}U, with the half-life time of 245,250 years, which decays to ^{230}Th **[**13**].** ^{238}U activity was determined indirectly from the gamma rays emitted by its daughter products (^{234}Th and ^{234m}Pa). The gamma-ray transitions of ^{228}Ac, ^{212}Bi and ^{208}Tl were used to evaluate the specific activity of ^{232}Th **[**15**]**.

^{226}Ra activity concentration was measured from 186.1 KeV after the subtraction of the 185.7 KeV of ^{235}U. The activity concentrations of ^{214}Pb and ^{214}Bi were measured from (295.1, 351.9) KeV and (609.3, 1120.3, 1238.1, 1764.5) KeV.

By subtracting the ^{235}U contribution calculated by γ-spectrometry, the 186 KeV multiple was corrected. As a result, ^{226}Ra activity can be calculated as follows:

$$\mathbf{A^{226}Ra = (N_{186} - A^{235}U * P_{185.7} * E_{185.7} * m * t) / (P_{186.2} * E_{186.} * m * t)} \quad (1)$$

Where N_{186} is the total count for the 186 KeV multiple, A ^{235}U is the activity of ^{235}U in Bq/Kg calculated from the activities of 143.8, 163.4 and 205.3 KeV, $P_{185.7}$ and $P_{186.2}$ are the emission probabilities of the 185.7 and 186.2 KeV lines of ^{235}U and ^{226}Ra, respectively, $E_{185.7}$ and $E_{186.2}$ are the detection efficiencies of the 185.7 and 186.2 KeV lines of ^{235}U and ^{226}Ra, respectively, m is the mass of the sample in Kg and t is the counting time in seconds [16].

For the actinium series gamma energies of 143.8 KeV, 163.4 KeV, 185.7 KeV and 205.3 KeV were taken to represent the ^{235}U concentrations. ^{40}K was determined directly from the 1460 KeV peak energy. ^{234}U activity was determined directly from the gamma rays emitted from this nuclide at energies of 53.2 KeV and 120.9 KeV is used [15].

The net count rate under the most prominent photo peaks of all radionuclide's are calculated from respective count rate after subtracting the background counts of the spectrum obtained for the same counting time. Then the activity of the radionuclide is calculated from the background subtracted area of prominent gamma ray energies. Activity of radium, thorium and potassium is calculated using the following equation:

$$\mathbf{Activity\ (Bq/Kg) = Net\ area / (T * \xi * M * I_\gamma)} \quad (2)$$

Where Net area is the net detected counts under a given peak area corresponding to the energy E, T is total counting time in seconds, ξ is counting the efficiency of the detector, M is Mass of sample in Kg and I_γ is intensity of the gamma spectral. The permissible activity levels for all types of sedimentary rocks are 32, 33, 45 and 412 Bq/kg for ^{238}U, ^{226}Ra, ^{232}Th, and ^{40}K respectively **[**17**]**.

2.4 Radiation Hazard Indices

Estimation of γ-radiation dose

The assessment of the radiation doses in humans from natural sources is very important. The absorbed dose is used to compare the amount of ionization induced by gamma rays in air to the extent of biological harm caused in

© 2021 NSP
Natural Sciences Publishing Cor.

living tissue in the radiation field [18]. The absorbed dose rate of one meter above the ground level owing to the concentration of Ra-226, Th-232 and K-40 is given by **[7]**:

$$D_{out} = K_{Ra} A_{Ra} + K_{Th} A_{Th} + K_K A_K \quad (3)$$

Where D_{out} is the outdoor absorbed dose rate (nGy/h) and A_{Ra}, A_{Th} and A_K are the activity concentrations of ^{226}Ra, ^{232}Th and ^{40}K respectively expressed in Bq/kg. Also, K_{Ra}, K_{Th} and K_K are the conversion factors (or dose rate coefficients) expressed in (nGy/hr per Bq/Kg) for Radium (0.462), Thorium (0.604) and potassium (0.042) respectively, the world's average value of D_{out} is 59 nGy/h **[19].**

Annual effective dose rate (outdoor) (AED) $_{out}$

AED (annual effective dose rate) (outdoor) $(AED)_{out}$ is calculated using the outdoor external dose rate (D_{out}), time spent in the outdoors (OF = 20% of 8760 hours in a year), and the conversion factor (CF = 0.7 Sv/Gy) to convert the absorbed dose in air to effective dose. The annual effective dose rate was calculated during the current analysis $(AED)_{out}$ in units of mSv per year is calculated by the following formula from **[17]**:

$$(AED)_{out}\ (mSv\ y^{-1}) = D_{out}\ (nGy/\ h) * 8760(h/\ y) * 0.2 * 0.7\ (Sv/\ Gy) * 10^{-6} \quad (4)$$

The world's average value of the annual outdoor effective dose rate is 0.07 mSv/ y **[19]**.

Excess lifetime cancer risk (ELCR)

The following formula was used to measure the excess lifetime cancer risk (ELCR) based on annual effective dose values:

$$ELCR_{outdoor}\ (mSv) = AED * 66 * 0.05 \quad (5)$$

Where 66 years is the period of life and 0.05 is the fatal cancer risk factor per Sievert **[20]**, the world average value of $ELCR_{outdoor}$ is $0.29 * 10^{-3}$ Sv = 0.29 mSv.

External hazard index (H_{ex})

The external hazard index (H_{ex}) due to the released γ– rays of the concentration materials samples is measured and analyzed using the following criteria:

$$H_{ex} = A_{Ra} / 370 + A_{Th} / 259 + A_k / 4810 \leq 1 \quad (6)$$

Where: ARa; ATh and AK are the activity concentrations (Bq/kg) of Radium, thorium and potassium in samples, respectively [21]

Annual gonadal dose equivalent (AGDE)

The organs of interest by UNSCEAR include the thyroid, the lungs, bone marrow; bone surface cell, the gonads and the female breast. Using the formula below, the annual gonadal dose equivalent (AGDE) attributable to the individual activities of ^{226}Ra, ^{232}Th, and ^{40}K can be determined.

$$AGDE\ (mSv/\ y) = 3.09A_{Ra} + 4.14A_{Th} + 0.314A_K \quad (7)$$

Where the world average value of (AGDE) is 300 mSv/y **[**17,22**].**

2.5 Radon mass exhalation rate and emanation coefficient

The emanation coefficient of the samples was estimated with γ -spectroscopy, by measuring γ rays from the radon decay daughter products, ^{214}Pb or ^{214}Bi **[**23**]**. Assuming an equilibrium state,

$$A_{Ra} = A_D + A_{Rn} \quad (8)$$

Where A_{Ra} is the measured activity of ^{226}Ra, A_D is the measured activity of the daughter elements ^{214}Pb or ^{214}Bi and A_{Rn}: is the estimated activity of ^{222}Rn, which disseminates throughout the environment A_{Rn} can be expressed using the radon emanation factor F, which is specified as

$$F = A_{Rn} / A_{Ra} = (A_{Ra} - A_D) / A_{Ra} \quad (9)$$

The mass exhalation rate or radon mass exhalation rate is the product of the emanation coefficient and 222Rn production rate [24]. The mass exhalation rate (E_{Rn} in Bq / Kg s) was determined through the following equation:

$$E_{Rn} = A_{Rn} A_{Ra} \lambda_{Rn} \quad (10)$$

Where, A_{Rn} is specific activity of ^{222}Rn in (Bq/Kg), A_{Ra} is the specific activity of ^{226}Ra in (Bq/Kg) and λ_{Rn} is the decay constant of ^{222}Rn ($2.1*10^{-6}$ s^{-1}).

Radon concentration was converted in to an effective dose, because the long-standing exposure to high concentration of radon and its progenies may lead to pathological effects like lung cancer. The annual effective dose received by workers due to inhalation of radon gas and its decay products, where calculated by the following equation:

$$AED_{Rn} = (A_{Rn} * 0.4 * K * H) / (3700\ Bq/m^3 * 170h) \quad (11)$$

$$A_{Rn}\ (Bq/m^3) = (A_{Ra} - A_D) * \rho \quad (12)$$

Where ρ is the density of radon (9.73 kg/m^3), AED_{Rn} is the annual effective dose of radon (mSv/y), A_{Rn} is the emanation coefficient of radon (Bq/m^3), K is the ICRP dose conversion factor 5 mSv WLM^{-1} for occupational worker and 3.88 mSv WLM^{-1} for general public, H is the annual occupancy at the location 2160 h for workers and 7000 h for residents (80 % of total time) and 170 is exposure hours taken for WLM^{-1} (Working Level Month). Where, the World average value of AED_{Rn} is (10 mSv) recommended by **[**25**]**.

3 Results and Discussion

3.1 Specific Activities

The average activity concentration of the radionuclides, ^{238}U ^{226}Ra, ^{232}Th and ^{40}K in the sedimentary rock samples

© 2021 NSP
Natural Sciences Publishing Cor.

under investigation is given in **Table (2)**. The activity concentration by Bq/ kg for ^{238}U, ^{226}Ra, ^{232}Th and ^{40}K varied from [717.09±21.51 to 6819.65±204.59], [842.86±25.28 to 9666.95±290.01], [29.85±0.89 to 170.46±5.11] and [345.38±10.36 to 856.54±25.70], respectively in the samples studied in the present work. The radioelement's World average values are 32 Bq/kg for ^{238}U, 33 Bq/kg for ^{226}Ra, 45 Bq/kg for ^{232}Th and 412 Bq/kg for ^{40}K **[**17**].**

The activity concentrations of all studied samples for ^{226}Ra and ^{238}U are also higher than the acceptable limit, as are the activity concentrations of all studied samples for 232Th, with the exception of sample (FAZ 1), and the activity concentrations of all studied samples for ^{40}K. (FAZ 3, FAZ 8).

Owing to the gaseous nature of its daughter radon, which has a half-life of 3.8 days, radium is the most harmful decay product of uranium. The alpha particles emitted by radon cause radiation damage to the lungs when inhaled through sedimentary rock dust. These findings point to a rise in radium activity levels.

In this work the activity ratios ^{238}U/^{235}U, ^{226}Ra/^{238}U was calculated for all samples see **Table (2)**. The activity ratio ^{238}U/^{235}U for all samples varies between (20.28 and 21.68) and the average is 21.3, which shows a good agreement with the normal ratio (21.7). The activity ratio ^{226}Ra/ ^{238}U ranging between (1.31 to 2.15) > 1, which show disequilibrium between ^{226}Ra and ^{238}U, this indicating preferential migration in for ^{226}Ra that indicate an alkaline solution as media of migration **[**1**].**

3.2 Radiological Hazard Indices

In order to assess the health effects, the radiation hazards of natural radioactivity in the samples, such as, absorbed dose rate (D_{out}), annual effective dose rate (outdoor) (AED) $_{out}$, excess lifetime cancer risk (ELCR), external hazard indices (H_{ex}) and annual gonadal dose equivalent (AGDE) associated with the radionuclide's were calculated and compared with internationally recommended values as shown in **Table (3)**.

The absorbed dose rate (D_{out}) (nGy/h) for all analyzed samples related to the behavior of ^{238}U,^{232}Th, and ^{40}K in the samples was measured and ranged from (454.12 to 4587.20) nGy/h, according to (Table 3). The values of the absorbed dose rate, which ranged from (0.56 to 5.62) mSv/y and (1.84 *10^{-3} to 18.56 *10^{-3}) Sv respectively for all studied samples, were used to measure the Annual effective dose rate (outdoor) $(AED)_{out}$ (mSv/y) in air and the amount of Excess lifetime cancer risk (ELCR) (Sv). All result are higher than the world average value 59 nGy/h for D_{out} , 0.07 mSv/y for $(AED)_{out}$ and 0.29*10^{-3} Sv for ELCR **[**17**]**.

Since ^{226}Ra has the highest activity concentration, it contributes the most to the absorbed dose rate in air, followed by ^{238}U, ^{40}K, and finally ^{232}Th. The contribution of ^{226}Ra, ^{238}U, ^{232}Th, and ^{40}K to the absorbed dose rate in air in the study region is depicted in the graph below (Fig. 3). ^{226}Ra accounts for 58% of the absorbed dose rate in air, ^{238}U, ^{40}K and then ^{232}Th account for 34%, 7% and 1% respectively. Also, the value of external hazard indices (H_{ex}) due to terrestrial gamma rays at 1m above the ground were varies from (2.65 to 26.87) Bq/kg which is higher than unity. This result points to a dangerous effect in that region for human health.

The value of Annual gonadal dose equivalent (AGDE) (mSv/y) related to the activity of ^{238}U,^{232}Th and ^{40}K in the samples was calculated for sedimentary rock sample and ranged from (3067.9 to 30719.8) mSv/y, all results are higher than the world average value 300 mSv/y **[**17**].** This means that these sedimentary rocks are not safety for human beings from the environmental radiation.

3.3 Radon Exhalation Rates

The annual effective dose from radon (AED_{Rn}) is represented by the activity concentration of ^{222}Rn, radon emanation factor F, radon mass exhalation rate, and radon mass exhalation rate Table **(4)** .The activity concentrations of ^{222}Rn were varied between (304.33– 5458.02) Bq/Kg, The values of the radon emanation factor and the radon mass exhalation rate of the samples are ranged from (0.21 to 0.71) and (538.67 to 109019.54) mBq/Kg.s, respectively.

We discovered that Fig. **(4)** Shows a strong correlation between ^{226}Ra and ^{222}Rn mass exhalation rate E_{Rn} in (mBq/Kg s) with correlation coefficient. (R^2= 0.853), which means that ^{222}Rn and ^{226}Ra accompanied each other, i.e. the highest ^{226}Ra activity has the higher value of E_{Rn} (109019.54 mBq/Kg s) as it clear in sample **FAZ 5**.

In the samples, the annual effective dose from radon AEDRn ranged from 50.84 to 911.84 mSv/y, with the highest value in sample FAZ 8 and the lowest value in sample FAZ 7. The results show that the Farsh El Azraq region in Sinai has high levels of annual effective dose from radon. All the samples in this locality were higher than the average world dose (10 mSv) recommended by **[**25**]** as showed in **Fig. (5).**

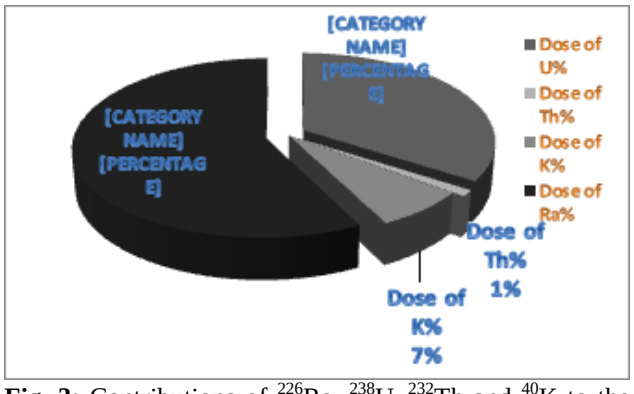

Fig. 3: Contributions of ^{226}Ra, ^{238}U, ^{232}Th and ^{40}K to the absorbed dose rate in air in the study area.

© 2021 NSP
Natural Sciences Publishing Cor.

Table 2: Average Specific activity concentration (Bq/kg), Activity ratios for sedimentary rock samples and Permissible level (P.L).

Sample No	^{226}Ra	^{235}U	^{238}U	^{232}Th	^{40}K	$^{238}U/^{235}U$	$^{226}Ra/^{238}U$
FAZ 1	5778.29±173.34	111.53±3.34	2404.53±72.13	29.85±0.89	428.74±12.86	21.55	2.40
FAZ 2	1630.28±48.90	57.50±1.72	1246.34±37.39	52.45±1.57	625.26±18.75	21.67	1.31
FAZ 3	3918.15±117.54	117.31±3.51	2524.38±75.73	75.19±2.25	410.67±12.32	21.51	1.55
FAZ 4	4075.40±122.25	103.34±3. 1	2095.97±62.87	62.97±1.89	493.60±14.80	20.28	1.94
FAZ 5	9666.95±290.01	324.30±9.7	6819.65±204.59	170.46±5.11	434.39±13.03	21.03	1.42
FAZ 6	1953.60±58.60	55.58±1.66	1205.29±36.16	124.68±3.74	856.54±25.70	21.68	1.62
FAZ 7	842.86±25.28	33.94±1.01	717.09±21.51	64.84±1.94	612.94±18.39	21.13	1.17
FAZ 8	7699.26±230.98	165.82±4.97	3576.36±107.29	95.16±2.85	345.38±10.36	21.57	2.15
FAZ 9	3355.44±100.66	122.32±3.66	2602.96±78.09	96.13±2.88	619.24±18.58	21.28	1.29

Table 3: The average values of Absorbed dose rate (D_{out}), Annual effective dose rate (outdoor) $(AED)_{out}$, Excess lifetime cancer risk (ELCR), External hazard indices (H_{ex}) and Annual gonadal dose equivalent (AGDE) for sedimentary rock sample with the World average value.

Sample No	**D_{out} (nGy/h)**	**$AED_{(out\ door)}$ (mSv/y)**	**ELCR (Sv)**	H_{ex} (Bq/kg)	**AGED (mSv/y)**
FAZ 1	2705.48	3.32	10.94×10^{-3}	15.82	18114.34
FAZ 2	810.94	0.99	3.28×10^{-3}	4.74	5453.13
FAZ 3	1872.72	2.29	7.58×10^{-3}	10.96	12550.33
FAZ 4	1941.45	2.38	7.86×10^{-3}	11.36	13011.18
FAZ 5	4587.20**	5.62**	18.56×10^{-3} **	26.87**	30719.80**
FAZ 6	1013.59	1.24	4.10×10^{-3}	5.94	6826.74
FAZ 7	454.12*	0.56*	1.84×10^{-3} *	2.65*	3067.91*
FAZ 8	3628.94	4.45	14.69×10^{-3}	21.25	24296.94
FAZ 9	1634.09	2.00	6.61×10^{-3}	9.57	10964.57
World average value	**59 (nGy/h)**	**0.07 (mSv/y)**	**0.29×10^{-3} (Sv)**	**1**	**300 (mSv/y)**

*The lowest value **The highest value

© 2021 NSP
Natural Sciences Publishing Cor.

Table 4: The average values of the activity concentration of radon ^{222}Rn (Bq/Kg), radon emanation factor, radon mass exhalation rate (mBq/Kg s) and the average annual effective dose (mSv/y) from radon AED_{Rn} for Sedimentary rocks samples.

Sample No	Rn^{222} (Bq/Kg)	F_{Rn}	E_{Rn} (mBq/Kg s)	AED_{Rn} (mSv/y)
FAZ 1	1196.80	0.21*	14522.48	199.94
FAZ 2	579.06	0.35	1982.45	96.74
FAZ 3	2600.27	0.66	21395.35	434.41
FAZ 4	2596.81	0.64	22224.39	433.84
FAZ 5	5370.26	0.55	109019.54**	897.18
FAZ 6	879.41	0.45	3607.84	146.92
FAZ 7	304.33*	0.36	538.67*	50.84*
FAZ 8	5458.02**	0.71**	88247.77	911.84**
FAZ 9	1567.81	0.47	11047.35	261.92

*The lowest value **The highest value

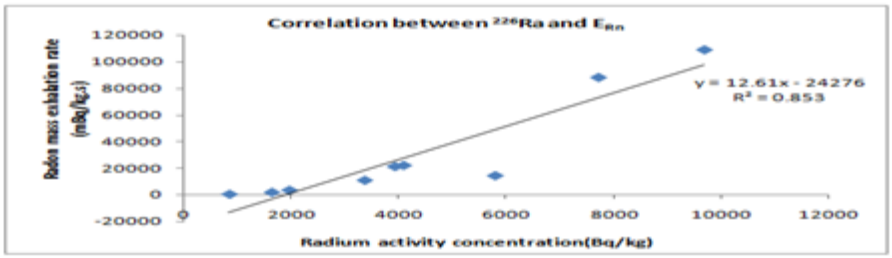

(Fig4) Correlation between Radon mass Exhalation rate E_{Rn} (mBq/Kg s) and activity of ^{226}Ra (Bq/Kg) for all samples.

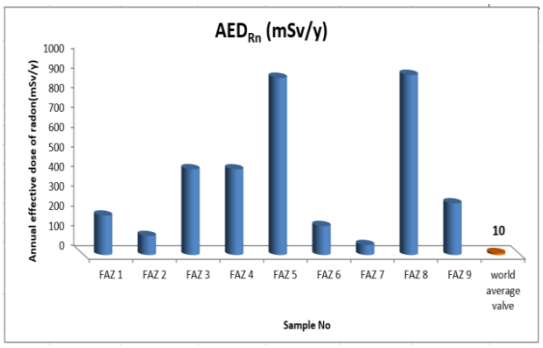

Fig. 5: The annual effective dose from radon AED_{Rn} in all samples and the World average value.

3.4 Comparison of the Average Activity Concentrations of ^{238}U, ^{226}Ra, ^{232}Th, and ^{40}K with Values from other Studies Worldwide

In order to infer the degree of similarity or differences, the average activity concentration of different radionuclides obtained from sedimentary rocks in this study are compared with other works in Egypt and other workers around the world **Table (5)**.

According to **[**32**],** the world wide average value of activity concentration for ^{238}U, ^{232}Th,^{40}K are 8-160 Bq/kg (mean value 32 Bq/kg), 4-130 Bq/kg (mean value 40 Bq/kg) and 100 -700 Bq/kg (mean value 420 Bq/kg), respectively. Sedimentary rocks in this study were greater than the world wide average value.

It is important to note that the values shown are not representative values for the countries mentioned, but only for the regions in which the samples were collected, The findings also showed that natural environmental radioactivity and subsequent external gamma radiation exposure are mainly influenced by geological and geographical conditions, and that they occur at different levels in the soils and rocks of different parts of the world [3].

4 Conclusions

The activity concentrations of all studied samples for ^{226}Ra and ^{238}U are also higher than the acceptable limit, as are the activity concentrations of all studied samples for ^{232}Th

© 2021 NSP
Natural Sciences Publishing Cor.

except sample (FAZ 1) and the activity concentrations of all studied samples for ^{40}K are higher than the permissible limit, with the exception of sedimentary rocks samples (FAZ 3, FAZ 8) from the Farsh El Azraq region in Sinai (FAZ 3, FAZ 8).

The activity ratio $^{226}Ra/^{238}U$ is greater than unity for all studied samples which show disequilibrium between ^{226}Ra and ^{238}U, this indicating preferential migration in /or accumulation of uranium. The average activity ratio $^{238}U/^{235}U$ for all samples shows a good agreement with the normal ratio (21.7).

The dose rate and external hazard index have high values. The ELCR factor assessed during this work on the basis of outdoor effective dose (E_{out}) was found to be higher than the permissible level. The values obtained shown a higher contribution from uranium and actinium series and therefore an annual effective dose higher than world average limit. In these sites, all of the measured samples show elevated levels of annual effective dose from radon.

This may indicate that the workers receive higher total effective doses due to high radioactivity, and this can result in significant radiation exposure, therefore the studied sedimentary rocks are not safety for human being from the environmental radiation. To minimize the risk, staff in these areas must take all necessary precautions and protective measures against the high levels of radioactivity. It can also not be used as a construction material due to its radioactive potential.

References

[1] D. Porcelli, P. W. Swarzenski The behavior or U- and Th-series nuclides in groundwater. In: Bourdon, B., et al. (Eds.), Reviews in Mineralogy and Geochemistry: Uranium Series Geochemistry, vol. 52. Mineralogical Society of America, Washington DC, pp. 317-361; 2003.

[2] N. Walley El-Dine. Study of natural radioactivity and the state of radioactive disequilibrium in U-series for rock samples, North Eastern Desert, Egypt. Appl. Radiat. Isotope., **66**, 80-85(2008).

[3] P. Elles, S. Y. Radionuclide-contaminated soil: a mineralogical perspective for their remediation. In: Dixon JB, Schulze DG (eds) Soil mineralogy with environmental applications, Chap 25. Soil Sci Soc of America, Madison., 737–763(2002).

[4] I.E. El Aassy, N. H. Botros, A. Abdel Razik, H. Sherif, A. Al Moafy, S. Aita, R. El Terb, A. S. Al Shami, Report on the Prospection and Proving of Some Radioactive Occurrences in West Central Sinai, Egypt. Internal Report, Nuclear Materials Authority, Cairo., 1986.

[5] M. El Sharkawi, M. El Aref, A. Abdel Mottelib, Manganese deposits in Carboniferous paleokarst profile, Um Bogma region, west central Sinai, Egypt. Miner Deposit., **25**,. 34–43(1989).

[6] I. E. El Aassy, F.Y. Ahmed, S.Y. Afifi and A.S. El Shamy, Uranium in laterites, Southwestern Sinai, Egypt. In: First seminar on nuclear raw materials and their technology, Cairo, Egypt, 1–3 Nov 1999, 1–20(1999).

[7] I. E. El Aassy, M. El Galy Mohamed, A. Nada Afaf, G. El Feky Mohamed, M. Abd El Maksoud Thanaa, M. Talaat Shadia, M. Ibrahim Eman, "Effect of alteration processes on the distribution of radionuclides in uraniferous sedimentary rocks and their environmental impact, southwestern Sinai, Egypt", Journal of Radioanalytical and Nuclear Chemistry., **289(1)**,. 173-184(2011).

[8] S. M. El-Bahi, A. Sroor, Y. Gehan Mohamed, N. S. El-Gendy, "Radiological impact of natural radioactivity in Egyptian phosphate rocks, phosphogypsum and phosphate fertilizers", Applied Radiation and Isotopes., **123**, 121-127(2017).

[9] G. F. Knoll, "Radiation detection and measurement", 3rd ed, Univ of Michigan. John Wiley and Sons. Inc. New York, ISBN: 0-471-07338-5(2000).

[10] Z. B. Alfassi, N. Lavi, The Dependence of The Counting of Efficiency of Marinelli Beakers for Environmental Samples on the Density of the Samples", Applied Radiation and Isotopes., **(63)**, 87-92(2005).

[11] International Atomic Energy Agency. Preparation and Certification of IAEA Gamma Spectrometry Reference Materials, RGU-1, RGTh-1 and RGK-1. International Atomic Energy Agency. Report-IAEA/RL/148, IAEA 1987.

[12] R. M. Anjos, R. Veiga, T. Soares, A. M. A. Santos, J. G. Aguiar , MHBO Frasca, J.A.P. Brage, D. Uzeda, L. Mangia, A. Facure, B. Mosquera, C. Carvalho , PRS Gomes. Natural Radionuclide Distribution in Brazilian Commercial Granites. Radiation Measurements., **(39)**, 245-253(2005).

[13] M. Pekala, J.D. Kramers and H.N. Waber, "234U/238U Activity Ratio Disequilibrium Technique for Studying Uranium Mobility in the Opalinus Clay at Mont Terri", Switzerland. Appl Radiat Isot., (**68)**, 984–992(2010).

[14] S. Stoulos, M. Manolopoulou, C. Papastefanou, Assessment of natural radiation exposure and radon exhalation from building materials in Greece. J Environ Radioact., **(69)**, 225–240(2003).

[15] Technical Reports Series No.295. Measurement of Radionuclides in Food and the Environment. A Guidebook, IAEA, Vienna-Austria, 1989.

[16] F. Saidou, J. P. Bochud, M. G. Laedermann, K. Njock, P. Froidevaux, "Radioactivity and Radiation Measurements, A Comparison of Alpha and Gamma Spectrometry for Environmental Natural Radioactivity Surveys. Applied Radiation and Isotopes., **(66)**, 215-222(2008).

[17] UNSCEAR, United Nations Scientific Committee on the Effect of Atomic Radiation, Sources and Effects of Ionizing Radiation, Report to General Assembly with Scientific Annexes, United Nations, and New York, 2010.

[18] Wedad Rayif Alharbi, Adel G. E. Abbady and A. El-Taher., Radon Concentrations Measurement for groundwater Using Active Detecting Method American Scientific Research Journal for Engineering, Technology, and Sciences (ASRJETS)., **14 (1)**, 1-11(2014).

[19] E. S. Abd El Halim, A. Sroor, S. M. El Bahi, I. E. El Aassy, M. El Shaikh Enass and K. M. Musa, "Assessment of Radioactivity levels and hazards for some sedimentary rock samples in different localities southwestern, Sinai, Egypt", International Journal of Recent Scientific Research., **8(11)**, 21916-21922(2017).

[20] E. S. Abd El-Halim, A. Sroor, N. Walley El-Dine, I. E. El-Aassy, M. Enass El-Sheikh and M. Naima Al-kbashy, "Radiological impact of natural radioactivity and excessive lifetime cancer risk in Egyptian phosphate rocks along Red Sea, Egypt", IOSR Journal of Applied Physics., **11(1)**, 47-57 (2019).

© 2021 NSP
Natural Sciences Publishing Cor.

[21] NCRP Report No. 93. Ionizing Radiation Exposure of the Population of the NEA – OECD (Nuclear energy agency). Exposure to radiation from natural radioactivity building materials, report by NEA group export, OECD. Paris., 1979.
[22] A. Hesham, I. Yousef Hamed, K. A. Mira Korany, "Assessment of Radiological Hazard Indices in Abu Rusheid Area, South Eastern Desert, Egypt, Using Gamma Ray Spectroscopy", Arab Journal of Nuclear Sciences and Applications., **52(2)**, 132-141(2019).
[23] K. G. Ioannides, T. J. Mertzimekis, C. A. Papachristodoulou and C. E. Tzialla, "Measurements of Natural radioactivity in phosphate fertilizers", Science of the Total Environment., **196(1)**, 63-67(1997).
[24]Abdulaziz Alharbi and A. El-Taher., Measurement of Natural Radioactivity and Radiation Hazard Indices for Dust Storm Samples from Qassim Region, Saudi Arabia. Life Science Journal., **11(9)**, 236-241(2014).
[25] International Commission on Radiological Protection. Protection against radon-222 at home and work, ICRP Publication 65. Oxford: Pentagon press, ICRP., 1993.
[26] F Alshahri, Atef El-Taher and AEA Elzain., Measurement of radon exhalation rate and annual effective dose from marine sediments, Ras Tanura, Saudi Arabia, using CR-39 detectors. Romanian Journal of Physics., **64**, 811(2019).
[27]A. kkurt and K. Gunoglu. "Natural Radioactivity Measurements and Radiation Dose Estimation in Some Sedimentary Rock Samples in Turkey", Hindawi Publishing Corporation. Science and Technology of Nuclear Installations, Article ID 950978., **(6)**, 2014.
[28] Q. M. Rashed-Nizam, M. K. Tafader, M. Zafar, M. M. Rahman, AKMSI Bhuian, R. A. Khan, M. Kamal, M. I. Chowdhury and M. N. Alam, "Radiological risk analysis of sediment from Kutubdia Island, Bangladesh due to natural and anthropogenic radionuclides", International Journal of Radiation Research.,**4(14)**, (2016).
[29] Isinkaye, Matthew Omoniyi, "Natural radioactivity levels and the radiological health implications of tailing enriched soil and sediment samples around two mining sites in Southwest Nigeria", Radiation Protection and Environment., **36(3)**, 122-127(2013).
[30] S Alashrah and Atef El-Taher., Assessing Exposure Hazards and Metal Analysis Resulting from Bauxite Samples Collected from a Saudi Arabian Mine. Polish Journal of Environmental Studies., **27(3)**, 959-966(2018).
[31] Sami Abd El Nabi, Nabil EL-Faramawy, Zeinab Morsy, Eman Salem, "Natural Radioactivity Measurement in Sedimentary Rock Samples Collected from the Bahariya Oasis, Western Desert, Egypt", JAKU: Earth Sci., **(23)**, 125-139, DOI: 10.4197/Ear.23-1.8, 2012.
[32] UNSCEAR, United Nations Scientific Committee on the Effect of Atomic Radiation. Sources, Effects and Risk of Ionizing Radiation, 2000.
[33] F. Alshahri, Atef El-Taher and Abd Elmoniem Ahmed Elzain., Characterization of Radon Concentration and Annual Effective Dose of Soil Surrounding a Refinery Area, Ras Tanura, Saudi Arabia. Journal of Environmental Science and Technology., **10(6)**, 311-319(2017).

© 2021 NSP
Natural Sciences Publishing Cor.